



*Int. J. New. Chem.*, 2021, Vol. 8, Issue 4, pp. 515-536.

## International Journal of New Chemistry

Published online 2020 in <http://www.ijnc.ir/>.

Open Access



Print ISSN: 2645-7237

Online ISSN: 2383-188x

### Original Research Article

## Synthesis of polyphenolic mesoporous nanocomposite for removal of acid dye from aqueous media: Adsorption studies Adsorption studies of anionic dye on polyphenolic mesoporous compound

Alireza Golshan Tafti<sup>1</sup>, Abosaeed Rashidi<sup>1,\*</sup>, Mohammad Esmail Yazdanshenas<sup>2</sup>, Habib-Allah Tayebi<sup>3</sup>

<sup>1</sup> Department of Textile Engineering, Science and Research Branch, Islamic Azad University, Tehran, Iran

<sup>2</sup> Department of Textile Engineering, Yazd Branch, Islamic Azad University, Yazd, Iran

<sup>3</sup> Department of Textile Engineering, Qaemshahr Branch, Islamic Azad University, Qaemshahr, Iran

Received: 2020-05-30

Accepted: 2020-09-30

Published: 2021-10-05

### ABSTRACT

The aim of this study is immobilization of mesoporous silica by tannin (tannin@SBA-15) for removal of acid blue 62 from aqueous media and determines the adsorption isotherm, thermodynamic and kinetic parameters. The characterization of adsorbent was carried out by different techniques such as Fourier-transform infrared spectroscopy (FT-IR), X-ray diffraction (XRD), N<sub>2</sub> adsorption/desorption, scanning electron microscope (SEM) and transmission electron microscope (TEM). UV-Vis spectrophotometer was also applied to determine the amount of remaining dye in the solution. The Effect of some parameters such as pH, adsorbent dosage and contact time for removal of acid blue 62 was examined and optimized at temperatures ranging from 25 to 45 °C. For determining the type of Isotherm model, Langmuir, Freundlich and Temkin were used and for attaining the Thermodynamic parameters such as changes in Gibbs free energy ( $\Delta G$ ), enthalpy ( $\Delta H$ ), and entropy ( $\Delta S$ ), Vant Hoff equation were applied. Optimum values were pH of 2, contact time of 90 min and absorbent dosage of 0.03 g. The Langmuir isotherm model showed very good agreement with the equilibrium data with maximum adsorption capacity of 1000 mg/g. The thermodynamic analysis also revealed that the adsorption process was feasible, spontaneous and exothermic. The results also indicated that the adsorption of acid blue 62 onto Tannin-aminated SBA-15 follows the pseudo-second order kinetic model. Tannin@SBA-15 has a good potential for acid blue 62 dye adsorption from aqueous media.

**Keywords:** SBA-15, Polyphenol, Acid dye, Adsorption Isotherm, Thermodynamic

## Introduction

Today, industrial effluents are removed of dyes and pollutants by using several techniques. Adsorption is regarded as one of the most useful and also functional physicochemical techniques. Some of the most critical factors for adsorption systems are high adsorption capacity of adsorbent and high-speed kinetics [1-5]. Various kinds of dyes like dyestuffs textiles, paper, plastics and pharmaceuticals are utilized by industries [6-11]. The environment is affected by the dyes reduced because most of them are poisonous and carcinogenic. Aqueous media are best removed of pollutants by cheap substances such as agricultural wastes which contain large amounts of polyphenols [6,12]. Researchers have studied some adsorption characteristics of natural plants such as pumpkin seed hull [13], garlic peel [14], rice husk activated carbon [15], and potato plant wastes [16]. An appropriate and efficacious adsorbent for the adsorption of contaminants from aquatic environment is a natural plant that contains large amounts of multiple phenolic hydroxyls called Tannin, since tannin is solved in water, there are some restrictions using it as the adsorbent in the aqueous solutions [17]. Therefore, in order to boost the performance of tannin for adsorption process, jellification and immobilization of it onto water insoluble materials such as silicates, collagen fiber, agarose and cellulose are done [18]. For many researches, tannin is not considered as an efficacious adsorbent, although it shows appropriate capacity. Bagd et all, researched Rosa Canina Galls for the adsorption of Basic Blue 9 and Basic Violet 3 on low-cost biosorbent [19]. In order to remove Pb (II) ions, a study was conducted by Meral Yurtsaver et all, on the adsorption features of modified quebracho tannin resin (QTR). This study indicated that QTR has high adsorption potential for Pb (II) ions and is considered a practical adsorbent [20]. To immobilize water-soluble groups, mesoporous materials consisted of large meso pores volume, high surface area and narrow pore size distribution were taken into account as efficacious and suitable insoluble supports. Grafting or in situ synthesis techniques are used for achieving surface modification of the mesoporous materials which is important in the adsorption capacity of mesopores. In addition, large specific surface area of the mesoporous materials will lead to homogeneous distribution of functional groups [21]. To remove the contaminants, different studies present surface modified mesoporous materials as efficacious substances. For removing Hg(II) from aqueous media, Shafiabadi et all, introduced the adsorption potential of polypyrrole modified SBA as nanocomposite [22]. Composites of natural polymer chitosan (CTS) and siliceous mesoporous SBA-15 were

synthesized by Qiang Gao et all, i.e. SBA-15/CTS (5%), SBA-15/CTS (10%) and SBA-15/CTS (20%) by pichydrolysis of tetraethyl orthosilicate when pore directing factor was present and succeeding cocondensation with a proper amount of CTS-based organosilane [23]. Asouhidou et all, prepared aminopropyl modified HMS (HMS-NH<sub>2</sub>) and  $\beta$ -cyclodextrin modified HMS (HMS-CD) in order to remove Remazol Red 3BS. It was revealed in this study that the adsorption potential of HMS-NH<sub>2</sub> and HMS was less than HMS-CD adsorbent [24]. Torabinezhad et all, studied the adsorption of Acid dye onto the amin-functionalized MCM-41 (NH<sub>2</sub>-MCM 41). They indicated that the adsorbent had a good potential for removing acid dye from aqueous media [25].

As stated before, tannin needs to be immobilized in water insoluble supports such as mesoporous materials in order that its solubility in aqueous media is prevented. Tannin-immobilized mesoporous silica (BT – SiO<sub>2</sub>) was synthesized by Xin Huang et all. They also studied the adsorption capability of this adsorbent to get rid of chromium cations from aqueous solution [26]. The activity and utilization of tannin as a useful adsorbent is inhibited by tannin low specific surface area. As a result, parallelism time enhances and it takes longer to reach parallelism status. Therefore, in order to prepare the appropriate adsorbent to associate in the adsorption procedure, uniform distribution of tannin on the surface of mesoporous silicate with high surface area is applied. So far, there have been no records about the synthesis of tannin modified mesoporous SBA-15. This study aims to provide tannin@SBA-15 mesoporous nanocomposite and also search about its adsorption capability to get rid of acid blue 62. Furthermore, in order to study the adsorption mechanism, isotherm, thermodynamic and kinetics of the adsorption process were investigated.

## Experimental

### Materials

Merck is the supplier for Tetraethyl orthosilicate (TEOS, SiC<sub>8</sub>H<sub>20</sub>O<sub>4</sub>), Pluronic P123 surfactant (SO<sub>20</sub>Po<sub>70</sub>EO<sub>20</sub>, M<sub>w</sub>=5800), tannic acid as source of polyphenol, (3-Aminopropyltriethoxysilane), glutaraldehyde (50%, w/w), hexane, HCl and NaOH for preparing of pH, Na<sub>2</sub>HPO<sub>4</sub> and

NaH<sub>2</sub>PO<sub>4</sub> for the preparation of buffer solution and deionized water. Furthermore, Dystar supplies acid blue 62 ( $\lambda_{\text{max}} = 620 \text{ nm}$ ). Fig.1 shows the chemical structure of acid blue 62.

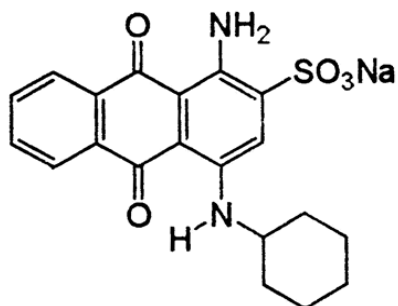


**Figure 1.** Chemical structure of Acid Blue 62

### Synthesis of mesoporous SBA-15

SBA-15 was synthesized according to Ghanei et all, as following [27]: 12 g of P123 as surfactant was solved in 90 mL of deionized water to make a clear solution. After that, 180 mL of HCl (2M) was added to the solution and stirred for 2 hours at 40 °C. It was allowed by adding 26.4 g of TEOS as a silica source and the resulting gel were stirred at 40 °C for 24 hours. Next step was heating the gel to 100°C for 48 hours. Filtering the solid product, washing it with water/ethanol and drying it for 24 hours at 100°C were also done. Eventually, the product was placed in the furnace for calcinations at 550°C for 5 hours for remove the current organics inside the as-synthesized mesoporous.

### Preparation of NH<sub>2</sub>-SBA-15

NH<sub>2</sub>-SBA-15 was synthesized according to Mirzaie et all, [28], at briefly: 2 g of SBA-15 and 10 mL of 3-aminopropyltriethoxysilane (APTES) were mixed and stirred with 50 mL of normal hexane under the reflux for 6 hours. Then, the prepared products were filtered, washed with acetone and deionized water and finally dried for 24 hours under vacuum at 323K.

## Synthesis of tannin@SBA-15 nanocomposite

Some covalent bonds can be made between electrophilic agents like glutaraldehyde and nucleophile agents such as phenolic rings of tannin. If tannin wants to be fixed on the surface of SBA-15, glutaraldehyde shows reactions as the cross-linking agent which contains amino group of NH<sub>2</sub>-SBA-15 and therefore a covalent bond is made. In order to prepare tannin SBA-15, nanocomposite requires blending 2 g of the ready NH<sub>2</sub>-SBA-15 with 1% tannin solution and then stirring the cocktail for 2 hours at room temperature and finally adding 6 mL of glutaraldehyde (50%, w/w) to it. Stirring the mixture for 24 hours at 298K is the next step. By filtering the mixture, washing it with deionized water and drying in the oven at 323K, the brown tannin SBA-15 nanocomposite is gained. The calculation of tannin loading on the surface of NH<sub>2</sub>-SBA-15 is done according to the various concentrations of tannin solution before and after the loading, which can be calculated by ultraviolet-visible spectrophotometer (6310, JENWAY, UK). The outcome shows about 30% loading of SBA-15 by 1% tannin solution.

## Instrumentation

X-ray diffraction (XRD) analysis in the range of  $2\theta=0-10^\circ$  by applying refractometer (XRD, Philips instruments, Australia 35 kV, 28.5 mA, 25°C and copper anode as a radioactive source) is a good way to testify the crystallinity of the synthesized SBA-15. In order to find the degree of concentration of dye solutions, before and after the adsorption, UV-Vis spectrophotometer was applied. And based on the BET plot, the BET surface area was calculated. And also, according to the adsorption curve of N<sub>2</sub> adsorption-desorption isotherm by utilizing BJH method (Barrett, Joyner, and Halenda), pore size and pore volume distributions were calculated. In order to confirm the coverage of SBA-15 surface by tannin, fourier transform infrared spectrometry (FTIR, 8400 s, Shimadzu, Japan, KBr technique) in the wave number of 400 – 4000 cm<sup>-1</sup> was applied. The samples were analyzed morphologically via scanning electron microscope (SEM, HITACHI, S-4160) and transmitting the elctron microscope (TEM, CM120, PHILIPS, Holland, 150 kV).

## Adsorption studies

Batch conducted a series of experiments in a shaker incubator that controlled the shaking speed by shaking of 250 mL Erlenmeyer flasks which contained 100 mL of dye solutions with primary concentrations of 40 up to 600 mgL<sup>-1</sup>. Every Erlenmeyer possessed optimal amount of tannin@SBA-15 powder in the optimum pH. The effects of some parameters such as pH, adsorbent amount, contact time and temperature on the dye removal were investigated. After 5, 15, 30, 45, 60, 90 and 120 minutes of contact times, samplings for each concentration were done. Before the testing the residual amount of dye in solution, all samples were centrifuged at 5000 rpm for 30 minutes. In order to measure the non-adsorbed or the balance concentration of dye, ultraviolet-visible spectrophotometer was used. The following equations were used to measure the adsorption capacity and removal efficiency, respectively:

$$q_t = ((C_i - C_t) \times V) / M$$

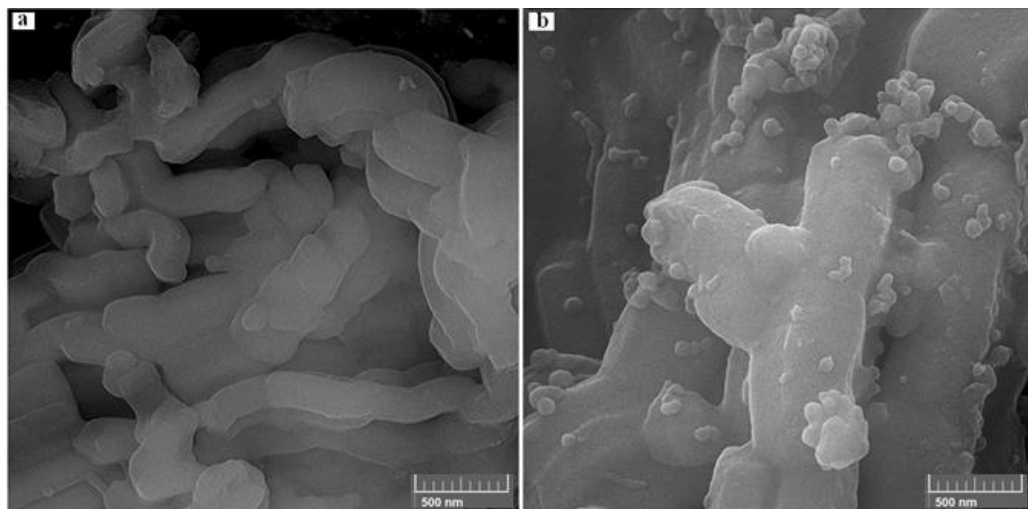
$$\text{Removal efficiency (\%)} = ((C_i - C_t) / C_i) \times 100$$

Where adsorption capacity at time  $t$  is shown by  $q_t$  (mg/g), and dye concentrations at initial and time  $t$  are represented by  $C_i$  and  $C_t$  respectively and  $V$  and  $M$  stand for the volume of dye solution (L) and mass of adsorbent (g).

## Results and Discussions

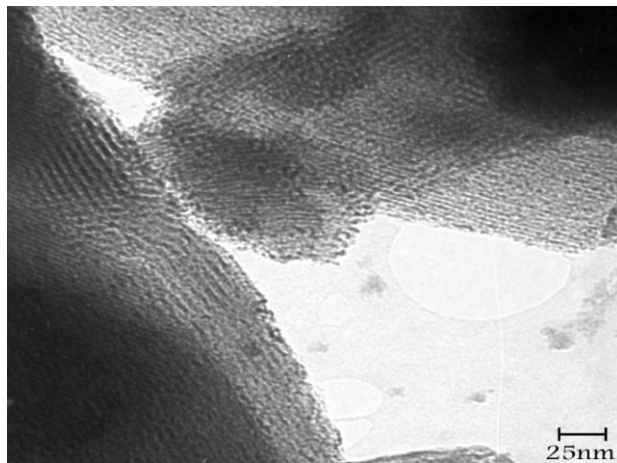
### Characterization analysis

Figure 2 illustrates the SEM images of SBA-15 and tannin@SBA-15. It is observable in the figure that tannin and composite are made in the form of fine and homogenous particles.



**Figure 2.** SEM images of SBA-15 (a) and Tannin-aminated SBA-15 (b)

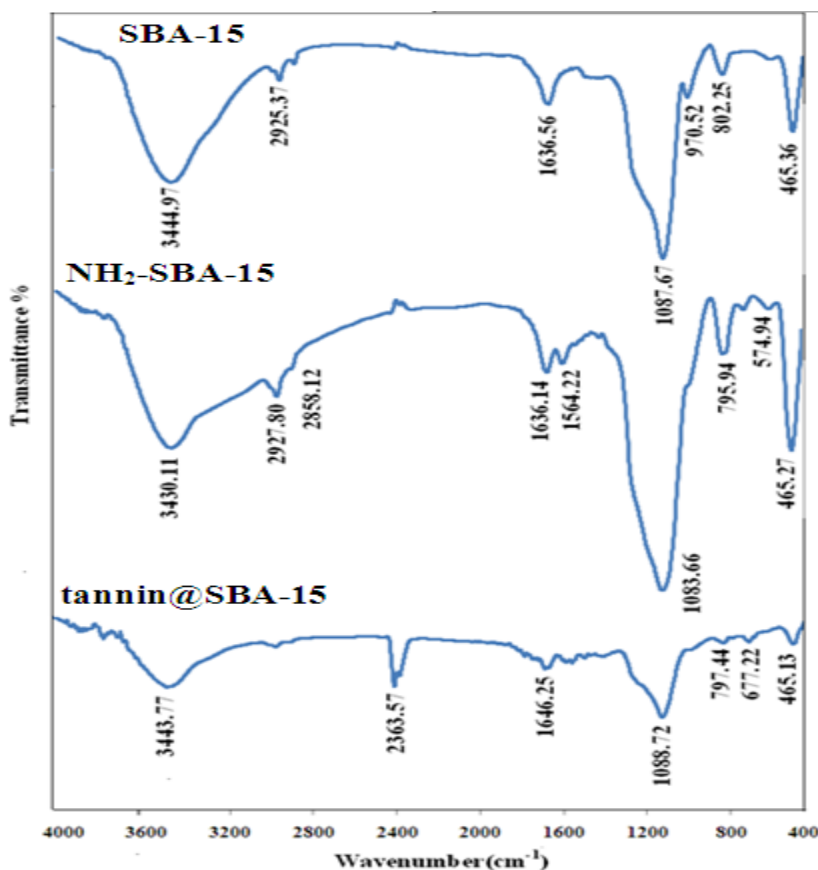
Figure 3 delineates the morphology of synthesized SBA-15 which is characterized by TEM images. TEM image depicts the Hexagonal well-organized mesoporous structure which was previously studied by Akbartabar et all, [29]. In this figure, 8 nm estimation is given for the pore size diameter of SBA-15 which was also verified by BET analysis.



**Figure 3.** TEM image of SBA-15

In order to prove the presence of tannin and amine on the SBA-15, FTIR analysis was conducted in range of  $400 - 4000\text{ cm}^{-1}$  (Figure 4). The presence of Si-OH group can be inferred from a broad band in the scope of  $3000 - 3700\text{ cm}^{-1}$  in figure 4.  $1087\text{ cm}^{-1}$  sharp acme verifies that asymmetric stretch vibrations of Si-O bond in Si-O-Si and reacts the peak at  $465\text{ cm}^{-1}$  and  $802\text{ cm}^{-1}$  are associated with the bending and symmetric stretch vibrations of Si-O-Si, respectively. A

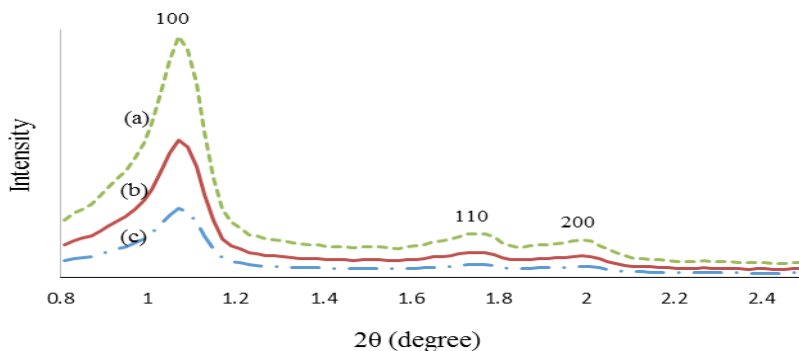
broad band in the scope of  $3000 - 3700 \text{ cm}^{-1}$  shows the stretching vibrations of  $-\text{OH}$  (phenolic and alcoholic groups) in tannin structure like  $-\text{OH}$  groups in the hydrogen-bonded of water in the case of synthesized composite (tannin@ SBA-15). Stretching vibrations of aromatic C-H and methylene ( $-\text{CH}_2-$ ) is shown at the peak up  $2925 \text{ cm}^{-1}$ . The sharp peak at  $2363 \text{ cm}^{-1}$  is the result of the presence of carboxyl group compound. Furthermore, the existence of aromatic rings is shown in the peaks in the scope of  $1450-1650 \text{ cm}^{-1}$ . Stretching vibrations of C-O-C indicate the absorption band at  $1088 \text{ cm}^{-1}$ , and the formation of SBA-15 powders is confirmed by the decrease of peak intensities in the scope of  $3000 - 3800 \text{ cm}^{-1}$  and at  $1087 \text{ cm}^{-1}$ .



**Figure 4.** FT-IR spectra of the SBA-15,  $\text{NH}_2\text{-SBA-15}$  and tannin@SBA-15

Figure 5 illustrates the low angle XRD models of synthesized SBA-15  $\text{NH}_2\text{-SBA-15}$  and tannin@SBA-15 in the scope of  $0 < 2\theta < 10$  with three peaks: a strong and sharp peak (100) at  $0 < 2\theta < 1$  and two weak peaks (110) and (200) at  $1 < 2\theta < 3$  that show the hexagonal order of synthesized silicate mesoporous material. There will be no changes in the XRD model due to the loading of SBA-15 by tannin and amine because of the filled channels of SBA-15 pores by

tannin and amine, the noticeable decrease of peak intensities for tannin@SBA-15 occurs. Furthermore, it can easily be found from the decrease in BET, volume and pore size of tannin@SBA-15 that amine and tannin entered the channels of SBA-15 [22]. The pore size of SBA-15 was calculated about 8.2 nm (BJH method) is smaller than the d spacing 9.3 nm for plane (100) of XRD pattern. So, XRD includes also thickness of silica walls.

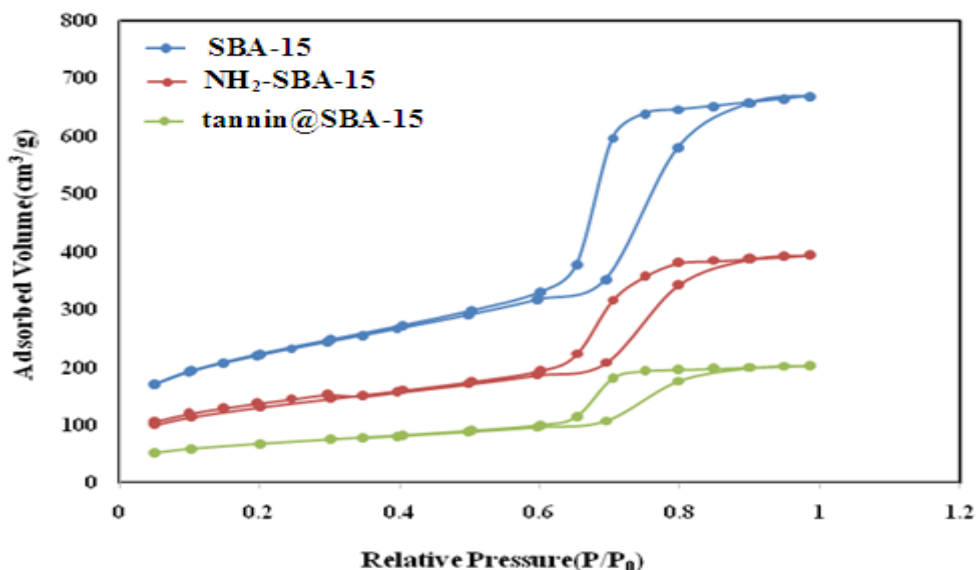


**Figure 5.** XRD patterns of (a) SBA-15, (b) NH<sub>2</sub>-SBA-15 and (c) tannin@SBA-15

In N<sub>2</sub> adsorption-desorption isotherm, isotherm of type IV with a hysteresis characterize are shown in figure 6 for all of the samples. P/P<sub>0</sub> = 0.6 – 0.8 shows a sharp rise in the adsorbed N<sub>2</sub> as a feature of mesoporous materials. The average pore size of 8.2 nm and a narrow pore size distribution are characterized for SBA-15 from what BJH method shows. Table 1 indicates the BET surface area, pore volume and average pore diameter of SBA-15 and also synthesized nanocomposites. It can clearly be seen that because of the decrease of BET surface area, volume and pore size of aminated SBA-15 and tannin@SBA-15 nanocomposites, the amine and tannin have entered into the channels of SBA-15. After loading by amine and tannin, the result is indicative that the SBA-15 BET surface area is depleted from 714.5 m<sup>2</sup>g<sup>-1</sup> to 390.7 and 199.2 m<sup>2</sup>g<sup>-1</sup> which eventually cause pore obstruction and the decrease of the BET surface area and pore size distribution of the synthesized adsorbent which is shown in table 1. The stuck of tannin particles in channels and the formation of hydroxyl functional group that could be absorbed by AB62 on SBA-15 surface are indicative of the reduction in pore size of tannin@SBA-15 [30].

**Table 1.** BET parameters of SBA-15, NH<sub>2</sub>-SBA-15 and tannin@SBA-15

Sample	Surface area (BET) (m <sup>2</sup> /g)	Pore diameter (nm)	Pore Volume (BJH) (cm <sup>3</sup> /g)
<b>SBA-15</b>	714.5	8.2	0.98
<b>Aminated SBA-15</b>	390.7	5.2	0.68
<b>Tannin-aminated SBA-15</b>	199.2	2.4	0.38

**Figure 6.** N<sub>2</sub> adsorption-desorption isotherms of SBA-15, NH<sub>2</sub>-SBA-15 and tannin@SBA-15

## Adsorption studies

### Effect of pH

The experiment of pH optimization was done in the scope of 2-12 with the primary dye concentration of 40 ppm, 0.02 g of adsorbent dosage and contact time of 120 minutes. Figure 7 shows the utmost dye removal was experienced at pH=2. As a result, the surface of the adsorbent and tannin at lower pH will absorb H<sup>+</sup> and show positive charges. The utmost adsorption takes place between negative charges of dye molecules and the positive charges of the adsorbent

surface which is the result of strong electrostatic attraction at pH=2. When negative charges of the surface rise and the positive charge declines, higher pH is expected. Therefore, reduced adsorption capacity is also expected due to the electrostatic repulsion of the tannin negative charges and the anionic dye molecules enhancement, i.e. adsorption capacity is depleted because of the competition between OH<sup>-</sup> ions and anionic molecules of acid blue 62 in alkaline condition [31].

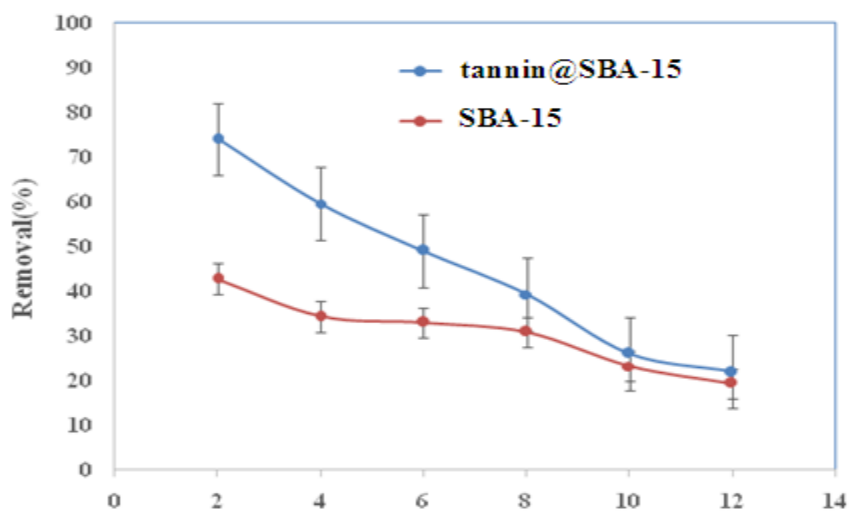


**Figure 7.** The effect of pH on dye removal percentage of SBA-15 and tannin@SBA-15

### Adsorption mechanism

The adsorption mechanism of acid blue 62 on tannin@SBA-15 is shown in figure 8. After ionic solubility of acid blue 62 in aqueous solution, positive and negative ions are released. Protons of media attack to the hydroxyl groups of tannin and form OH<sup>+2</sup> groups on the tannin structure. So, ion exchange occurs between the negatively charged acid blue 62 and positive charges of adsorbent.

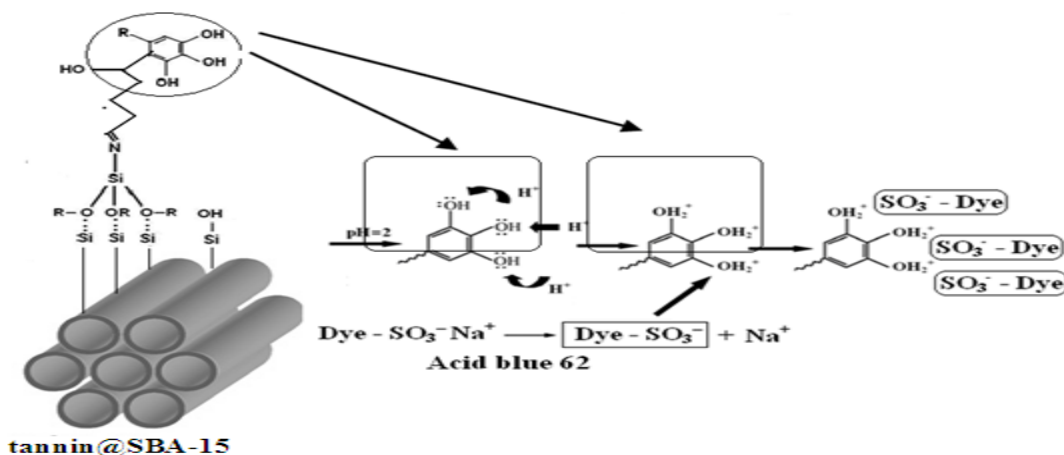


**Figure 8.** The proposed mechanism for adsorption of acid blue 62 onto tannin@SBA-15

### Effect of adsorbent dosage

Figure 9 depicts the influence of adsorbent amount on dye removal efficacy. As can be seen, with the increase of adsorbent up to the optimum value, the removal efficiency increases and after that, no change was observed. This phenomenon can be attributed to the extra accumulation of adsorbent in the solution and the reduction of the acceptor sites and inhibition of the adsorption process [32]. In this research, dosage experiments were carried out in the presence of 0.01 to 0.1g of adsorbent with the initial dye concentration of 40 ppm, pH of 2.0 at 25°C for 2 hours. The result showed that the optimum dosage of adsorbent was 0.03 g, which was consequently used in the other experiments.

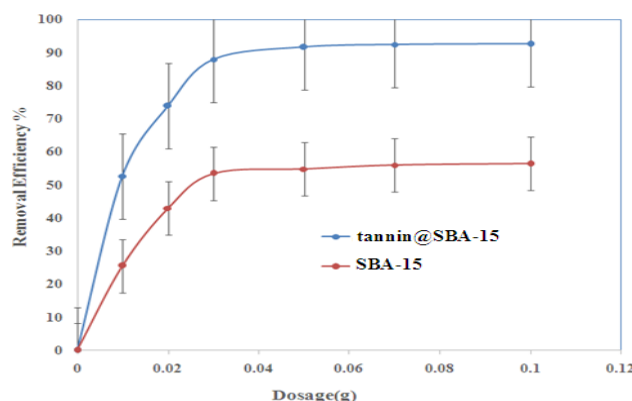


**Figure 9.** Effect of adsorbent dosage on the removal efficiency of acid blue 62

## Effect of contact time at different temperatures

Many experiments were done at different temperatures of 25°C, 35°C and 45°C at various time intervals from 5 to 120 minutes to investigate the impacts of temperature and contact time on the adsorption of acid blue 62. The adsorption procedure for all temperatures in the first 15 minutes can be immediately seen in figure 10. In fact, adsorption will be completed after 30 minutes and as a result the adsorption equilibrium will be achieved. Thus, the equilibrium time was set to 90 minutes contact time, which was used to other experiments, too. If contact time is increased, the accumulation of acid blue 62 on the adsorbent surface can occur. Therefore, dye molecules cannot deeply penetrate into the areas with higher energy. The single, smooth and persistent adsorption curves show that the saturation status and monolayer coverage of the adsorbent surfaces is satisfied through tannin@SBA-15. Furthermore, the rise of temperature up to 45°C is the result of reduction in adsorption capacity. In other words, the adsorption process sounds to be exothermic. This phenomenon can be associated with the nature of the adsorption process.

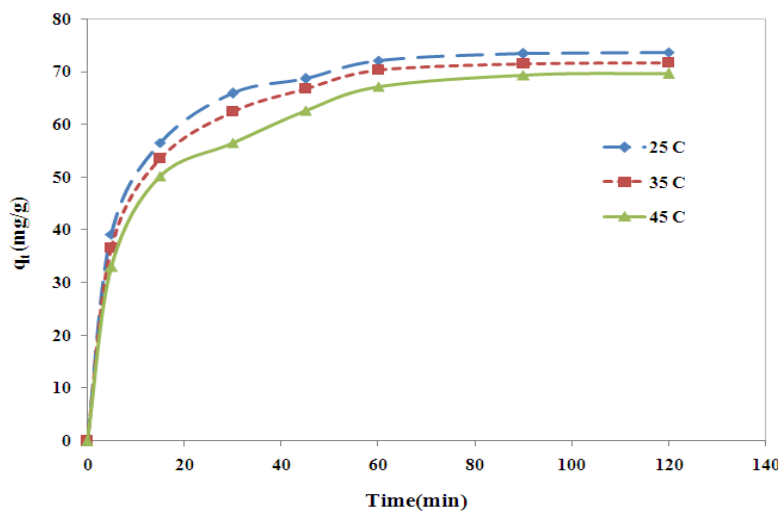


**Figure 10.** Effect of contact time and temperature on adsorption capacity (initial dye concentration: 40 ppm, adsorbent dosage: 0.03 g, pH of 2).

## Adsorption thermodynamic

Thermodynamic analysis is used to understand the nature and also the mechanism of adsorption process. By applying the following equations (such as Vant Hoff equation (6)), thermodynamic parameters such as  $\Delta G$ ,  $\Delta H$  and  $\Delta S$  can be calculated [33].

$$K_c = C_{Ae} / C_e \quad (4)$$

$$\Delta G = -RT \ln K_c \quad (5)$$

$$\ln K = \Delta S / R - \Delta H / RT \quad (6)$$

The equilibrium constant, the equilibrium concentration in solution (mg/L) and amount of adsorbed dye each liter of solution in the equilibrium condition is shown by  $K_c$ ,  $C_e$  and  $C_{Ae}$ , respectively.

The changes in Gibbs free energy, enthalpy and entropy are denoted by  $\Delta G$  (kJ/mol),  $\Delta H$  (kJ/mol) and  $\Delta S$  (J/mol.K), respectively. Furthermore, in order to gain the values of  $\Delta H$  and  $\Delta S$  the Vant Hoff equation (eq.6) was applied, and equation (5) was used to measure  $\Delta G$ . As the results of the study show in table 2 and figure 11, the temperature rise causes the decline in the adsorption of acid blue 62 on the composite. Therefore an exothermic adsorption process exists. In fact, by applying negative values of  $\Delta G$ , the possibility and spontaneity of the adsorption of acid blue 62 on tannin@SBA-15 is highlighted. Based on what table 2 denotes, negative values associated with Gibbs free energy are enhanced by increased temperature. As a result, the increase of temperature improves the spontaneity of the adsorption procedure. The negative value of the  $\Delta H$  shows that the adsorption is exothermic. Furthermore, the magnitude of  $\Delta H$  can specify the adsorption sorts. The adsorption of acid blue 62 on tannin@SBA-15 is categorized as the physical adsorption while the  $\Delta H$  is less than 21 kJ/mol and the involved forces appear to be weak [27]. The positive value of  $\Delta S$  in the interface of the solution-adsorbent through the adsorption procedure which supports the improved efficacy can cause increased irregularity. The positive value of  $\Delta S$  shows the reversible adsorption of acid blue 62 on tannin@SBA-15. The exothermically and irregularity of adsorption of many dyes on various adsorbent are frequently referred to by many researches [34].

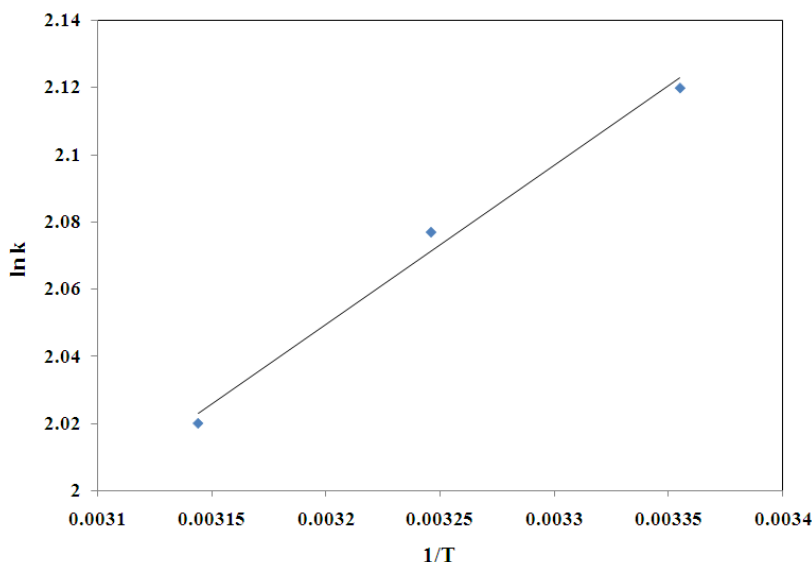


**Figure 11.** Effect of temperatures in the range of 25 to 45°C on thermodynamic parameters (initial dye concentration:40 ppm, adsorbent dosage: 0.03 g, pH of 2, contact time of 90 min).

**Table 2.** Thermodynamic parameters of the adsorbed acid blue 62 by tannin@SBA-15

Initial concentration (mg/L)	$\Delta H^\circ$ (kJ/mol)	$\Delta S^\circ$ (J/mol.K)	298 K		$\Delta G^\circ$ (kJ/mol)		R <sup>2</sup>	
			308 K	318 K	308 K	318 K		
40	-3.93	4.33			-5.25	-5.32	-5.34	0.99

## Adsorption isotherm models

The adsorption isotherm includes the interaction between adsorbent and adsorbate. Due to investigating the adsorption of acid blue 62 on Tannin@SBA-15 nanocomposite and designating the predominant isotherms, the experimental data were analyzed at 25°C.

### The Langmuir isotherm

The purpose of Langmuir isotherm is to determine the adsorption capacity which relies on monolayer adsorption on top of similarity of the active sites energy.

Langmuir enjoys the following non-linear forms

$$q_c = q_m K_L C_e / (1 + K_L C_e) \quad (7)$$

Adsorption capacity ( $\text{mg g}^{-1}$ ) is shown by  $q_e$  equilibrium concentration ( $\text{mg/L}$ ) by  $C_e$ , the maximum adsorption capacity of the adsorbent ( $\text{mg/g}$ ) by  $q_m$  and Langmuir constant by  $K_L$  which makes an association between the adsorbent and the adsorbate. The binding affinity of adsorbent for adsorption of dye molecules is represented by  $K_L$ .

## The Freundlich isotherm

The Freundlich isotherm is based on the experimental data that shows the heterogeneous surfaces (various adsorption energy of active sites) as follows:

$$q_c = K_F C_e^{1/n} \quad (8)$$

Assessment of the adsorption capacity ( $\text{Lg}^{-1}$ ) is shown by  $K_F$ , the adsorption intensity by  $n$  value and the heterogeneity of the adsorbent surface by  $1/n$ . As a matter of fact, high values of  $K_F$  represent the easy adsorptions while high values of  $n$  demonstrate the worthwhile adsorptions. The  $n$  values below the unity show the chemisorption process, the unity of  $n$  denotes the linear adsorption and the values of  $n$  in the range of 2-10 represent the favorable and physical adsorption.

## The Temkin isotherm

The Temkin isotherm was assessed with respect to the multilayer adsorption:

$$q_c = B \ln(AC_c) \quad (9)$$

The linear forms of three isotherms are shown in Figure 12. In order to calculate the basic parameters of isotherms, the linear regression was used (see table 3). Based on the compatibility between the experimental data and the results which were gained from isotherms, the ranks can be explained based on the  $R^2$  values as following:

Langmuir (0.991) > Temkin (0.953) > Freundlich (0.915)

From what table 3 shows, Langmuir isotherms denote the largest  $R^2$  value, which sounds to indicate to the monolayer adsorption of acid blue 62 on tannin@SBA-15. Moreover, from Langmuir isotherm, the uniform and homogenous distribution of adsorbate on the surface of nanocomposite can be inferred. It can be deduced from Freundlich isotherms that the value of 1.71 for  $n$  depicts the favorable adsorption. The correlation coefficient Langmuir isotherm is higher than that of Freundlich isotherm ( $R^2 = 0.915$ ). As a result, compared with the Freundlich isotherm in the case of consistency with the experimental data, it is Langmuir isotherm which is consistent. In order to study the multilayer adsorption, Temkin isotherm was also utilized.

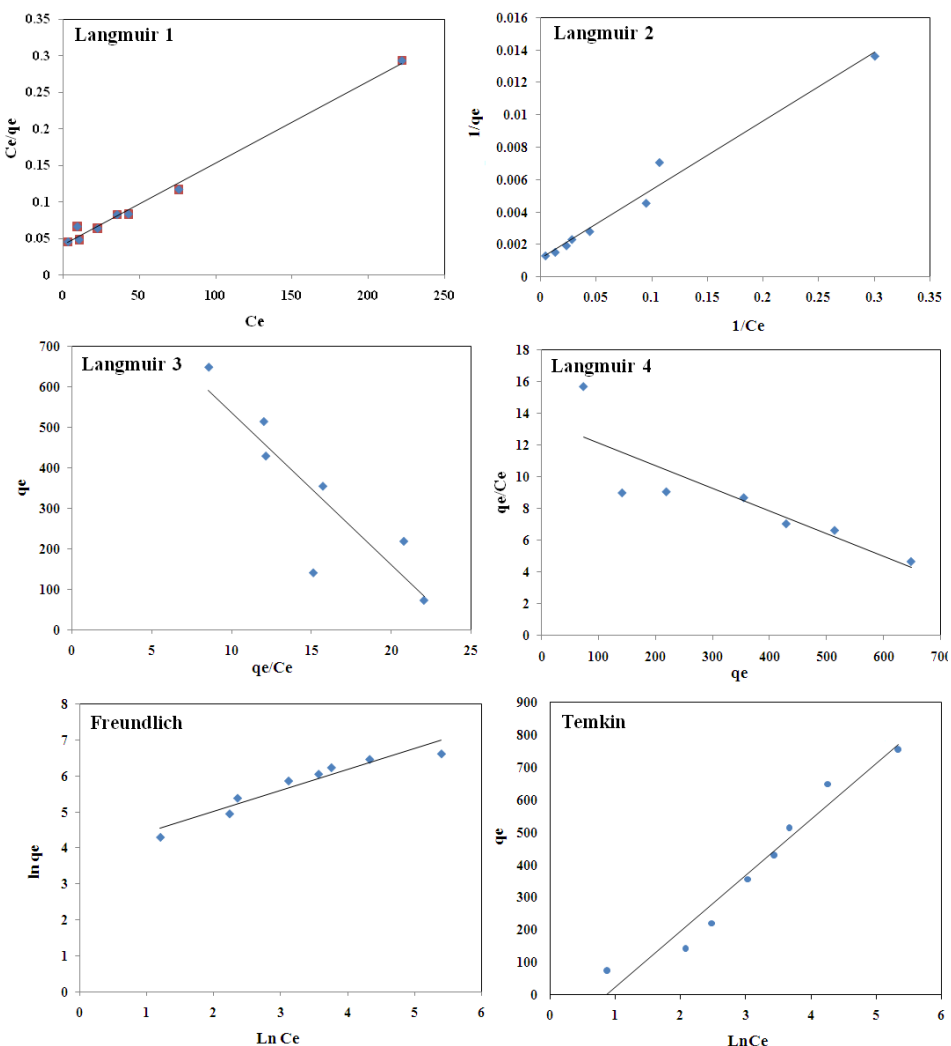


**Figure 12.** The linear forms of different isotherms at 298 K

Table 3 shows that  $R^2$  value of Temkin isotherm is reported to be lower than that of the Langmuir isotherm and it specifies the monolayer adsorption, and as a result, the Langmuir model is derived to be the superior isotherm.

**Table 3.** Parameters of different isotherm models

Isotherm	Non linear equation	Linear form	Parameter	$R^2$
Langmuir 1		$C_e/q_e = 1/k_L q_m + (1/q_m) C_e$ $C_e/q_e$ vs. $C_e$	$q_m=1000$ mg/L $K_L=0.025$ L/mg	<b>0.991</b>
Langmuir 2		$1/q_e = 1/k_L q_m C_e + 1/q_m$ $1/q_e$ vs. $1/C_e$	$q_m=1000$ mg/L $K_L=0.024$ L/mg	<b>0.979</b>
Langmuir 3	$q_e = q_m K_L C_e / (1 + K_L C_e)$	$q_e = q_m - q_e / k_L C_e$ $q_e$ vs. $q_e/C_e$	$q_m=912.4$ mg/L $K_L=0.026$ L/mg	<b>0.779</b>
Langmuir 4		$q_e/C_e = q_m/k_L - q_e/k_L$ $q_e/C_e$ vs. $q_e$	$q_m=970$ mg/L $K_L=71.43$ L/mg	<b>0.738</b>
Freundlich	$q_e = K_f C_e^{1/n}$	$\ln q_e = \ln K_f + 1/n \ln C_e$ $\ln q_e$ vs. $\ln C_e$	$n=1.71$ $K_f=46.71$ (mg/g). $(L/mg)^{1/n}$	<b>0.915</b>
Temkin	$q_e = B \ln (A C_e)$	$q_e$ vs. $\ln C_e$	$B=172.7$ J/mole $A=0.42$ L/g	<b>0.953</b>

A dimensionless parameter in the Langmuir isotherm is involved in  $R_L$ , which is considered as an efficient parameter and stated as follows:

$$R_L = 1/(1 + K_L C_o) \quad (10)$$

In the above equation, initial concentration and Langmuir constant are shown with  $C_o$  and  $K_L$  respectively. Table 4 demonstrates the adsorption type, categorized according to the  $R_L$  values. In addition, table 5 shows the  $R_L$  values measured through equation (10). It can be seen that the adsorption of acid blue 62 on tannin@ SBA-15 nanocomposite is considered to be favorable.

**Table 4.** Effect of  $R_L$  values on the adsorption quality

Adsorption quality		$R_L$
<b>Unfavorable adsorption</b>		$R_L > 1$
<b>Favorable adsorption</b>		$0 < R_L < 1$
<b>Irreversible adsorption</b>		$R_L = 0$
<b>Linear adsorption</b>		$R_L = 1$

**Table 5.** Values of  $R_L$  for the adsorption of acid blue 62 on tannin@SBA-15 at 298K and different initial concentrations

Initial concentration (ppm)	40	80	120	200	250	300	400	600
$R_L$	0.50	0.33	0.25	0.16	0.14	0.11	0.09	0.06

The adsorption of some dyes was studied on various silicate mesoporous supports for some comparative goals. The utmost monolayer adsorption capacities are shown in table 6. Compared to the others, the biggest value of  $q_m$  is for tannin@SBA-15 nanocomposite. In fact, high specific surface area of SBA-15, large amounts of phenolic groups in tannin structure and homogenous distribution of tannin on SBA-15 leads to increase of tannin@SBA-15 adsorption capacity.

**Table 6.** Comparison of maximum monolayer adsorption capacity on different SBA-15 basis adsorbents

Adsorbate	Adsorbents	$q_m$ (mg/g)	References
<b>Congo red</b>	3-aminopropyl-triethoxysilane functionalized SBA-15	234.9	[35]
<b>acid red 18 (AR18)</b>	natural polymer chitosan (CTS) / SBA-15	232.6	[23]
<b>Hg (II)</b>	polypyrrole/SBA-15	200	[22]
<b>Acid Blue 113</b>	pentaethylene hexamine functionalized SBA-3 (SBA-3/PEHA)	769.23	[36]
Acid blue 62	<b>Tannin-aminated SBA-15</b>	<b>1000</b>	<b>This study</b>

## Conclusion

In this study, the immobilization of tannin onto aminated hexagonal mesoporous silicate (SBA-15) was done. Then, as a new composite adsorbent, it was utilized to remove acid blue 62 from aqueous solution. High adsorption capacity (1000 mg/g) for the tannin@SBA-15 and a quick adsorption rate for the dye removal were among the findings of this study. Appropriate loading of SBA-15 by tannin and FTIR spectroscopy further confirmed the findings. Volume and average pore size from BJH method were obtained from the BET equation (based on the specific surface area); it was also found that tannin is well-distributed on the surface and on the pores of the adsorbent. As a result, one of the best adsorbent for removing the dye is the synthesized tannin@SBA-15. Moreover, the improved interaction between acid blue 62 and adsorbent was depicted which consequently led to the improved potential of dye removal. The indirect effect of the temperature on dye removal and an inverse relationship between the temperature at various concentrations and the amount of dye removal were also concluded. The fact that adsorption process was exothermic and spontaneous was also depicted. By applying Langmuir, Freundlich

and Temkin isotherms and parameters of each isotherm, the equilibrium data were examined; and by utilizing non-linear regression, the correlation coefficients were measured. Furthermore, according to the  $R^2$  values, the Langmuir adsorption isotherm model had the best correlation coefficient.

## References

- [1] K. Aghajani, H. A. Tayebi, *Fiber. Polym.*, 18, 3 (2017).
- [2] F. Z. Benhachem, A. Tarik, F. Bouabdallah, *Chem. Rev. Lett.*, 2, 33 (2019).
- [3] M. Chabane, D. Benamar, *Chem. Rev. Lett.*, 2, 118 (2019).
- [4] M. Nikpassand, L. Zare Fekri, *Chem. Rev. Lett.*, 2, 7 (2019).
- [5] Z. Sarikhani, M. Manoochehri, *Int. J. New. Chem.*, 7, 30 (2020).
- [6] E. Binaeian, N. Seghatoleslami, M. J. Chaichi, H. A. Tayebi, *Adv. Powder. Technol.*, 27, 4 (2016).
- [7] A. Rahmani, H. Rahmani, A. Zonouzi, *Int. J. New. Chem.*, 7, 169 (2020).
- [8] M. Mozafarjalali, M. Hajiani, A. Haji, *Int. J. New. Chem.*, 7, 111 (2020).
- [9] A. Saidfar, M. Alizadeh, S. Pirsa, *J. Chem. Let.*, 1, 39 (2020).
- [10] M. R. Jalali Sarvestani, S. Majedi, *J. Chem. Let.*, 1, 32 (2020).
- [11] H. Kalantary, M. Manoochehri, *Int. J. New. Chem.* (2020) DOI: 10.22034/ijnc.2020.121400.1113.
- [12] E. Binaeian, H. A. Tayebi, A. S. Rad, M. Payab, *Mater. Chem. Phys.*, 10, 185 (2017).
- [13] B. H. Hameed, M. I. El-Khaiary, *J. Hazard. Mater.*, 155, 3 (2008).
- [14] B. H. Hameed, A. A. Ahmad, *J. Hazard. Mater.*, 164, 2 (2009).
- [15] M. Shabandokht, E. Binaeian, H. A. Tayebi, *Desalin. Water. Treat.*, 57, 57 (2016).
- [16] N. Gupta, A. K. Kushwaha, M. C. Chattopadhyaya, *Arab. J. Chem.*, 9, 10 (2016).
- [17] M. Yurtsever, I. A. Şengil, *J. Hazard. Mater.*, 163, 1 (2009).
- [18] M. Özcar, I. A. Şengil, H. Türkmenler, *Chem. Eng. J.*, 143, 1 (2008).
- [19] E. Bağda, *Desalin. Water. Treat.*, 43, 1 (2012).
- [20] M. Yurtsever, I. A. Şengil, *J. Hazard. Mater.*, 163, 1 (2009).

- [21] M. Mirzaie, A. Rashidi, H. A. Tayebi, M. E. Yazdanshenas, *J. Polym. Environ.*, 26, 5 (2018).
- [22] M. Shafiabadi, A. Dashti, H. A. Tayebi, *Synthetic. Met.*, 212, 55 (2016).
- [23] Q. Gao, H. Zhu, W. J. Luo, S. Wang, C. G. Zhou, *Micropor. Mesopor. Mat.*, 193, 78 (2014).
- [24] D. D. Asouhidou, K. S. Triantafyllidis, N. K. Lazaridis, K. A. Matis, *Colloid. Surface. A.*, 46, 1 (2009).
- [25] A. Torabinejad, N. Nasirizadeh, M. E. Yazdanshenas, H. A. Tayebi, *J. Nanostructure Chem.*, 7, 3 (2017).
- [26] X. Huang, X. Liao, B. Shi, *J. Hazard. Mater.*, 173, 1 (2010).
- [27] M. Ghanei, A. Rashidi, H. A. Tayebi, M. E. Yazdanshenas, *J. Chem. Eng. Data.*, 63, 9 (2018).
- [28] M. Mirzaie, A. Rashidi, H. A. Tayebi, M. E. Yazdanshenas, *Phys. Chem. Res.*, 6, 3 (2018).
- [29] I. Akbartabar, M. E. Yazdanshenas, H. A. Tayebi, N. Nasirizadeh, *Iran. J. Health Sci.*, 5, 3 (2017).
- [30] I. Akbartabar, M. E. Yazdanshenas, H. A. Tayebi, N. Nasirizadeh, *Phys. Chem. Res.*, 5, 4 (2017).
- [31] A. Torabinejad, N. Nasirizadeh, M. E. Yazdanshenas, H. A. Tayebi, *Int. J. Nano Dimens.*, 7, 4 (2016).
- [32] E. Binaeian, H. A. Tayebi, A. Shokuh Rad, S. Afrashteh, *J. Macromol Sci.*, 55, 3 (2018).
- [33] H. Tayebi, M. E. Yazdanshenas, A. Rashidi, R. Khajavi, M. Montazer, *J. Eng. Fiber. Fabr.*, 10, 1 (2015).
- [34] M. Mirzaie, A. Rashidi, H. A. Tayebi, M. E. Yazdanshenas, *J. Chem. Eng. Data.*, 62, 4 (2017).
- [35] I. Laaz, M. J. Stébé, A. Benhamou, D. Zoubir, J. I. Blin, *Colloid. Surface. A.*, 490, 10 (2016).
- [36] M. Anbia, S. Salehi, *Dye. Pigment.*, 94, 1 (2012).

### How to Cite This Article

Alireza Golshan Tafti, Abosaeed Rashidi, Mohammad Esmail Yazdanshenas, Habib-Allah Tayebi, “**Synthesis of polyphenolic mesoporous nanocomposite for removal of acid dye from aqueous media: Adsorption studies Adsorption studies of anionic dye on polyphenolic mesoporous compound**” International Journal of New Chemistry., 2020; DOI: 10.22034/ijnc.2020.128383.1116.